Determination of Onset of Apoptosis in Granulosa Cells of the Preovulatory Follicles in the Bonnet Monkey (*Macaca radiata*): Correlation with Mitogen-Activated Protein Kinase Activities

Uma J[1], Muraly P[1], Shalu Verma-Kumar[1] and Medhamurthy R[1,2,3]

Department of Molecular Reproduction, Development and Genetics[1] and Primate Research Laboratory[3], Indian Institute of Science, Bangalore -560012, India

Short Title: Monkey granulosa cell apoptosis

Key Words: Ovary; Apoptosis; Follicular development; Granulosa cells; Signal transduction

Corresponding Author: R. Medhamurthy
Department of Molecular Reproduction, Development and Genetics
Indian Institute of Science
Bangalore -560012, India

Grant Support: This work was supported financially by Life Sciences Research Board, Indian Council of Medical Research and the DBT post-doctoral training program (SVK). Presented in part at the 12th National Conference on Recent Advances in Reproductive Health, Jaipur, India, 2003.

ABSTRACT

During reproductive life, only a selected few ovarian follicles mature and ovulate while vast majority of follicles undergo a degenerative process called atresia. Recent studies have indicated that follicular atresia is mediated through apoptosis of follicular granulosa cells. The objectives of the present study were to evaluate whether granulosa cells of preovulatory follicles in the monkey would undergo apoptosis and to correlate apoptosis with mitogen-activated protein (MAP) kinase activities. Bonnet monkeys undergoing controlled ovarian stimulation cycles were utilized for stimulation of multiple follicles and granulosa cells were retrieved from preovulatory follicles at 24, 48, 72 and 96 h after stopping of gonadotropin treatment. Serum and follicular fluid E_2 concentrations were highest at 24 h but declined precipitously ($p<0.05$) to reach the lowest concentrations at 96 h; and P_4 concentrations during this period however did not increase indicating the absence of luteinization. Quantitative analysis of genomic DNA by 3' end labeling revealed presence of low molecular weight fragments from 48 h onwards, but by agarose gel electrophoresis DNA laddering could be visualized only after 72 h. Messenger RNA expression for Bax, caspase-2 and caspase-3 increased with the onset of apoptosis. Immunoblot analysis of MAP kinases in lysates of granulosa cells (48-72 h) indicated increased ($p<0.05$) levels of phosphorylated ERK-1 & -2, JNK-1 & -2 and p38. However, in vitro kinase assay data indicated that only phospho- JNK and -p38 activities were higher at 72 h compared to that at 24 h. These results demonstrate that granulosa cells of preovulatory follicles undergo apoptosis and increased activities of phospho-JNK and -p38 are correlated with apoptosis in the primate.

INTRODUCTION

Tissue homeostasis is dependent on the proper relationships among cell proliferation, differentiation and cell death. Apoptosis (also referred to as programmed cell death) is a highly regulated process by which an organism eliminates unwanted cells. Apoptosis plays an important role in regulation of ovarian function in mammals (for reviews see [1-3]). Over the course of reproductive lifespan, only a selected few follicles mature and ovulate, while vast a majority of follicles i.e., up to 99%, do not grow to ovulate but degenerate during various stages of follicular development due to the process of initiation of apoptosis of granulosa cells [4-7]. The mechanism(s) by which only a few follicles (the number of which is more or less specific to each species) mature during each reproductive cycle, while many of the follicles undergo atresia, remains to be delineated. Although gonadotropins, FSH and LH, are primary regulators of ovarian follicular growth, the involvement of paracrine/autocrine factors originating within the ovary during the process of folliculogenesis has become increasingly apparent over the last few years [8]. For instance, several studies indicate that rapidly growing follicles produce higher levels of autocrine and paracrine growth factors that stimulate increases in vasculature and FSH responsiveness which may result in escape of these follicles from undergoing atresia [9, 10].

Although there is extensive data on characterization of apoptosis on the basis of morphological and biochemical changes that occur in the dying granulosa cells (reviewed in [1, 2], the sequence of signaling events that commit the granulosa cells to death remains to be characterized. Recent studies demonstrate the critical roles played by gonadotropins, steroids and growth factors in attenuation of follicular (granulosa)

apoptosis. One of the mechanisms by which these so called “survival factors” attenuate apoptosis in granulosa cells is by altering the expression of cell-death related genes ([6, 8] and for review see [11]). Moreover, mechanisms such as increased expression of survival factors and phosphorylation of critical phosphoproteins also play a important role in mediating the action of trophic growth factors on survival of cells (reviewed in [3]).

Among the major types of signal transduction pathways in eukaryotic cells are protein kinase cascades that culminate in activation of protein kinases known as mitogen-activated protein kinases or MAP kinases. In mammals, four major groups have been identified, and each of these groups of MAP kinase is activated by a protein kinase cascade (reviewed in [12]). They are extra-cellular response kinase (ERK), Jun N-terminal kinase (JNK), p38MAPK (p38) and the big MAPK (ERK5). The hallmark of MAPK signaling is the stimulation-dependent nuclear translocation of the involved kinases, which regulate gene expression and the cytoplasmic acute response to mitogenic, stress-related, apoptotic and survival stimuli. It has been shown that in Rat1 and PC12 cells, apoptosis induced by the withdrawal of trophic growth factors involves a rapid increase in p38, JNK and inhibition of ERK [13, 14]. However, FSH has been shown to activate ERK and p38 in granulosa cells in vitro [15-17]. These findings suggest that determination of survival and apoptosis is also critically regulated by MAP kinases. The present study was therefore, undertaken to determine the time of onset of apoptosis in granulosa cells retrieved from monkeys that received exogenous human gonadotropin preparations to promote growth of multiple follicles. Additionally, we sought to examine the role of MAP kinases during granulosa cell apoptosis.

MATERIALS AND METHODS

Reagents

The polyclonal antibodies specific to phospho-p38 MAPK (# 9211), phospho-SAPK/JNK (# 9251), phospho-p42/44 MAPK (# 9100), p38 MAPK (# 9212), ERK-1 (# sc-19), ERK-2 (# sc-154) and JNK-1 (# sc-571) were purchased from Cell Signaling Technology, Beverly, MA (# 9100, # 9211, # 9212, # 9251) and Santa Cruz Biotechnology Inc., Santa Cruz, CA (# sc-19, # sc-154, # sc-571 and # sc-572). In vitro kinase activity assay kit for p38 MAPK (# 9820) and protein kinase substrates for ERK (Elk-1 fusion protein, # 9184) and JNK (c-jun fusion protein, # 6093) were purchased from Cell Signaling Technology, Beverly, MA.

Omniscript RT was obtained from Quiagen, Valencia, CA while Taq DNA Polymerase, random hexamers, RNAsin and dNTPs were from Promega, Madison, WI. Oligonucleotide primers were synthesized by Sigma-Genosys (Cambridgeshire, UK). All other reagents were purchased from Sigma Chemical Co., St. Louis, MO, Gibco BRL, Gaithersburg, MD, or sourced locally.

Animal Protocols

All procedures involving monkeys in this study were cleared by the Institutional Animal Ethics Committee of the Indian Institute of Science. Adult female bonnet monkeys (*Macaca radiata*) weighing 3.1 to 5 kg with a history of regular menstrual cycles of 27-29 days were utilized for the study. The general care and housing of monkeys at the Primate Research Laboratory, Indian Institute of Science have been

described elsewhere [18]. During the study period, the temperature in the animal rooms supplied with fresh 5 μm filtered air ranged from 22-28°C (dry bulb temperature) and 17-22°C (wet bulb temperature) maximum and minimum, respectively. Studies were conducted during January to February and July to December months, since female bonnet monkeys exhibit summer amenorrhea during March through June months [18]. Monkeys were daily monitored for onset of menses. Starting from day 1 of menses, monkeys were treated with hFSH (25 IU Metrodin twice daily i.m.; 0900 and 1700 h, Ares Serono, Aubonne, Switzerland) for 6 days followed by hFSH plus hLH (25 IU each; Pergonal, twice daily i.m.; Ares Serono, Aubonne, Switzerland) for 2.5 days to promote multiple follicular growth and development. Blood samples were collected daily or on alternate days to estimate serum estradiol (E_2) and progesterone (P_4) for monitoring follicular growth during and following withdrawal of gonadotropin treatment. A variety of methods have been used to stimulate the growth and maturation of multiple follicles in a number of non-human primate species [19] and (reviewed in [20]). The protocol in the present study was similar (except for the lower dose and shortened duration of treatment) to the one reported by others [19]. To rule out that spontaneous endogenous LH surges did not occur during the course of gonadotropin treatment and withdrawal period, selected serum samples were analyzed for monkey LH concentration using a specific radioimmunoassay [21] and the results confirmed the absence of LH elevations during or after stopping of gonadotropin treatment. Also, serum and follicular fluid levels of P_4 were low indicative of absence of luteinization.

Collection and Processing of Granulosa Cells

Trans-abdominal ultrasonography (Aloka SSD500V equipped with a 7.5 MHz linear transducer, Aloka Co. Ltd. Tokyo, Japan) was performed for visual inspection of the follicle number and diameter on 10^{th} day after initiation of the treatment. It was consistently observed that 5-6 follicles per ovary of >5 mm could be identified. The follicular fluid was aspirated with the help of 25 gauze 1½″ needle attached to 1 ml syringe. As far as possible care was taken to aspirate the follicular contents from follicles >5 mm, and wherever possible efforts were made to flush the follicle after aspiration to maximize the yield of granulosa cells. For RNA isolation, follicular fluid was collected separately from one or two follicles and centrifuged at 290 g and the cell pellet was stored at -70°C until processed for RNA isolation. Immediately after collection, follicular fluid was centrifuged at 290 g for 7 min at 4^0C. The supernatant was discarded and the cell pellet was suspended in PBS solution. After counting the cells, the cell suspension was aliquoted and centrifuged again to obtain the cell pellet. One or two of the aliquots were snap frozen in liquid nitrogen and stored at -70°C until analysis and the remaining aliquot was subjected to cell lysate preparation as described below. When the follicular fluid was mixed with blood, it was collected separately into a separate test tube for further processing. The blood mixed follicular fluid was centrifuged at 290 g for 7 min, the cell pellet was suspended in 1 ml Percoll buffer [1X HBSS containing HEPES (0.252 g/100 ml) and 0.1% BSA] and the cell suspension was carefully layered over a 40% Percoll gradient and centrifuged for 30 min at 480 g. Granulosa cells were recovered from the interface, resuspended in 5 times their volume with Percoll buffer and centrifuged at 130 g for 10 min. The cell pellet was dissolved in PBS and centrifuged at

290 g for 7 min and the cell pellet was used for cell lysate preparation (see below) or stored at -70°C until analysis. The cell number was determined using haemocytometer and cell viability by 0.4% Trypan blue exclusion. The total number of cells recovered per retrieval ranged from $3.6x10^6$ to $10.5x10^6$ cells (per monkey/time at 24, 48, 72 or 96 h after stopping of gonadotropin treatment) with cell viability of 51 to 89 %.

Isolation of Genomic DNA and Analysis

Genomic DNA was extracted from granulosa cells, precipitated, dissolved in distilled water and spectrophotometrically quantitated as described previously for DNA fragmentation analysis [22, 23]. Genomic DNA (10 -15 µg for agarose electrophoresis or 500 ng for quantitative analysis) was either subjected to agarose gel electrophoresis, stained with ethidium bromide and DNA visualized by UV transillumination, or analyzed for quantitation of low molecular weight (LMW) DNA fragments as described previously [22, 23].

RNA isolation

Total RNA was extracted from granulosa cells using Trizol reagent according to the manufacturer's recommendations and quantitated spectrophotometrically. Analysis of RNA at OD A_{260} vs A_{280} consistently yielded a ratio above 1.8.

RT-PCR Analysis

RT-PCR was carried out using Peltier Thermal Cycler PTC-200 MiniCycler™ Instrument (MJ Research, Waltham, MA). Oligonucleotides used for PCR are listed in Table 1. Computer searches and sequence alignments were performed at

http://www.ncbi.nlm.nih.gov and http://searchlauncher.bcm.tmc.edu/. The identity of the PCR products was confirmed by sequence analysis. Total RNA (1 µg) was reverse transcribed using the following RT mixture: 200 µM of dNTPs, 10 units of RNAsin, 10 X RT buffer [250 mM Tris HCl (pH 8.3 at 25°C), 250 mM KCl, 50 mM $MgCl_2$, 2.5 mM Spermidine and 50 mM DTT], 10 µM of oligo dT and 4 units of Omniscript reverse transcriptase (Quiagen, Valencia, CA) in a total reaction volume of 20 µl. RNA was allowed to stand at 65°C in a water bath for 5 min before chilling on ice for 5 min. After addition of the RT mixture, reverse transcription was carried out for 1 h at 37°C. For PCR, cDNA equivalent to 500 ng total RNA was used. The PCR mix was made up of 200 µM of dNTPs, 1 X Taq buffer [50 mM KCl, 10 mM Tris HCl (pH 9.0 at 25°C), 1.5 mM $MgCl_2$ and 0.1% Triton X 100], 10 µM of each gene specific primer and 2 units of Taq DNA Polymerase, in a total reaction volume of 50 µl. Semi-quantitative multiplex RT-PCR was carried out as per the method of Wong et al. [24] with a few modifications and using the following cycling parameters: For caspase -2 and -3, an initial denaturation at 95°C for 2 min, 5 cycles of denaturation at 94°C for 45 sec, annealing at 65°C for 45 sec and extension at 72°C for 1 min; followed by 30 cycles of touchdown PCR with denaturation at 94°C for 45 sec, annealing from 65°C to 58°C for 45 sec and extension at 72°C for 1.5 min. The caspase-2 primers were dropped in to allow 30 cycles of amplification and RPLO primers were dropped into allow 18 cycles of amplification at annealing temperature of 58°C. This was followed by a final extension at 72°C for 10 min. Similarly for Bax, touchdown PCR was carried out with an initial denaturation at 95°C for 2 min, 5 cycles of denaturation at 94°C for 30 sec, annealing at 60°C for 30 sec

and extension at 72°C for 45 sec, followed by 30 cycles with denaturation at 94°C for 30 sec, annealing at 58°C for 30 sec and extension at 72°C for 1 min. The RPLO primers were dropped into allow 18 cycles of amplification for RPLO at annealing temperature of 58°C. The PCR products were separated on a 2% agarose gel containing ethidium bromide and photographed under UV using Alpha Imager 1200 Documentation and Analysis System (Alpha Innotech Corp., San Leandro, CA**).**

Preparation of Cell Lysates for Immunoblotting

Granulosa cell lysate was prepared following the previously published procedure [23]. In brief, an aliquot of washed cell pellet (~ 2 x10^6) was transferred to 150 µl of RIPA lysis buffer, sonicated using Branson Cell Disrupter at 20 % power for 10 sec, incubated for 30 min on ice with intermittent vortexing before centrifugation at 15000 g for 10 min at 4°C. The clarified supernatant was recovered, aliquoted and stored at -70°C until analyzed for various MAP kinases. The protein was estimated using Bradford method [27].

Western Blotting

Whole cell lysate (25-40 µg) was resolved by 10% SDS-PAGE and electroblotted onto PVDF membrane using a semi-dry transfer unit (Bio-Rad Laboratories, Richmond, CA) as described previously [23].

In vitro MAP kinase assays

Assays were carried out with few modifications of published procedures (ERK & JNK; [28, 29]) or according to the manufacturer's protocol (phospho-p38 MAPK). In

brief, 100-200 µg of granulosa cell lysate protein was incubated with either 20 µl of immobilized phospho-p38 MAPK antibody or phospho-JNK (1:200)/phospho-ERK (1:100) MAP kinase antibodies for overnight followed by additional incubation with 20 µl of Protein-A-Agarose for 3 h at 4^0C. The resultant immune complexes were collected by centrifugation at 15,000 g for 30 sec, and after washing, the immunoprecipitates were used directly in the assay. MAP kinase activities were assayed in the immune complexes using respective Glutathione-S-Transferase (GST) fusion proteins as substrates. For phospho-p38 MAP kinase activity assay, the immune complexes were washed in kinase buffer (25 mM Tris (pH 7.5), 5 mM β-Glycerophosphate, 10 mM $MgCl_2$, 2 mM DTT, 0.1 mM Na_3VO_4) and the pellet was resuspended in 50 µl of kinase buffer supplemented with 200 mM ATP and 2 µg ATF-2 fusion protein and incubated for 30 min at 30^0C. The reaction was terminated by adding 25 µl of 3X SDS sample buffer. Samples were separated on a 10% acrylamide gel, transferred to PVDF membrane and probed with phospho-ATF-2 antibody (1:1000). For phospho-JNK and ERK MAP kinase activity assays, the immune complexes were washed in kinase buffer and the pellet resuspended in 25 µl of kinase buffer supplemented with 20 µM ATP, 2.5 µCi γ^{32}P ATP and 2 µg GST-c-Jun (JNK assay)/or Elk-1 (ERK assay) fusion proteins and incubated for 30 min at 30^0C. The reaction was terminated by adding 12.5 µl of 3X SDS sample buffer, samples were separated on a 12% acrylamide gel, followed by gel drying and autoradiography.

Steroid Assays

Estradiol and P_4 concentrations in serum were determined by specific RIA reported previously [30]. The E_2 (GDN #244) and P_4 (GDN #337) antisera were kindly

provided by Professor G. D. Niswender, University of Colorado, Fort Collins, CO. Follicular fluid was diluted with 0.1% Gelatin-PBS before ether extraction and assay. The sensitivity of the assays for E_2 and P_4 were 39 pg/ml and 0.1 ng/ml, respectively. The inter- and intra-assay coefficients of variation for both the hormones were <10%.

Statistical Analyses

Data wherever applicable was expressed as mean ± SEM. The arbitrary densitometric units were represented as the percentage relative to control, which was set at 100%. The data were analyzed by one-way ANOVA followed by Newman-Keuls multiple comparison test (PRISM Graph Pad version 2, Graph Pad software Inc., San Diego, CA). P value of <0.05 was considered statistically significant.

RESULTS

Steroid concentrations in monkeys during and after gonadotropin treatment

Mean serum E_2 concentrations in monkeys receiving exogenous human gonadotropin treatments to promote multiple follicular growth are presented in Fig.1. Also shown in the Figure are serum E_2 concentrations at different time intervals after stopping of gonadotropin treatment. Serum E_2 concentrations increased slowly during the first 6 days of hFSH, but increased briskly after initiation of combination of hFSH and LH treatment to reach peak concentrations of 2920 ± 233.2 pg/ml at 24 h after stopping of gonadotropin treatment. Serum E_2 concentrations declined precipitously ($p<0.05$)

thereafter and the concentrations were 543 ± 99.7, 127 ± 17.6 and 65 ± 10.5 pg/ml at 48, 72 and 96 h after stopping of gonadotropin treatment, respectively. The follicular fluid concentrations of E_2 and P_4 on different days after stopping of gonadotropin treatment are shown in Fig. 2. The pattern of E_2 concentrations in the follicular fluid paralleled the serum E_2 patterns with high concentrations at 24 h but significantly lower ($p<0.05$) concentrations at 48, 72 and 96 h after stopping of gonadotropin treatment. Follicular fluid P_4 concentrations tended to be lower at 48, 72 and 96 h compared to that at 24 h (Fig. 2). Based on E_2 (and P_4) secretory pattern the duration of experimental period was arbitrarily divided into two phases, proliferation and non-proliferation phase, and represented with a log scale Y-axis in Fig. 3. Also shown in Fig. 3 is the pattern of P_4 concentrations on different days after stopping of gonadotropin treatment. Serum P_4 concentration was lowest ($p<0.05$) at 96 h compared to 24 h. It is evident that E_2 concentrations decreased following withdrawal of gonadotropin treatment and P_4 concentrations did not increase suggesting the absence of differentiation of granulosa cells.

Biochemical analyses of apoptosis

Agarose gel electrophoresis and ethidium bromide staining of genomic DNA isolated from granulosa cells retrieved at different time intervals after stopping of gonadotropin treatment showed characteristic pattern of DNA laddering indicative of presence of apoptotic granulosa cells at 72 and 96 h (Fig. 4A). At 24 h, there was no evidence for DNA laddering, and at 48 h although there was no appearance of DNA ladder, there was evidence of smearing of DNA (Fig. 4A). When genomic DNA was

analyzed for LMW fragments by 3' end labeling, the results showed presence of LMW DNA fragments which could be visualized in granulosa cells retrieved at 48, 72 and 96 h after stopping of gonadotropin treatment (Fig. 4B). Quantitation of DNA fragments indicated that the LMW DNA fragments increased ($p<0.05$) 300-700% during 48 to 96 h compared to that at 24 h (Fig. 4C).

Bax mRNA was detectable in granulosa cells retrieved at 24 h after stopping of gonadotropin treatment (Fig. 5A). The Bax mRNA expression tended to be higher ($p>0.05$) at 48 and 72 h, but the expression was significantly higher ($p<0.05$) at 96 h compared to the 24 and 48 h time points. Fig. 5B depicts the expression patterns of caspase-2 and capase-3 at different time intervals after stopping of gonadotropin treatment.

Caspase-2 & -3 mRNAs were detectable in granulosa cells retrieved at 24 h and progressively increased, but the caspase-3 expression increased only 50% at 96 h compared to the 24 h time point. On the other hand, during the corresponding period, caspase-2 expression increased nearly 2 fold (Fig. 5B).

Correlation of MAP kinase activities during granulosa cell apoptosis

Figure 6 shows representative immunoblots and integrated arbitrary densitometric unit data of phospho (p)- and total- ERK-1 & -2 levels (expressed as a percentage of results obtained at 24 h) from granulosa cells retrieved during 24-96 h after stopping of gonadotropin treatment. p-ERK-1 & 2 levels were higher at 48 h, but were significant ($p<0.05$) at 72 h. Total ERK-2 levels although slightly higher at 48 and 72 h, but not statistically significant from the 24 h time point. On the other hand, total ERK-1 levels

showed increase that mirrored its phospho-levels. Granulosa cell lysate from 24 and 72 h were subjected to in vitro ERK assay and the result did not confirm the increased phospho-levels observed by immunoblot analysis (Fig. 6).

Representative immunoblots and integrated arbitrary densitometric unit data of p-JNK-1 & 2 and total JNK-1 are shown in Figure 7A. p-JNK-1 levels increased significantly ($p<0.05$) at 48 and 72 h after stopping of gonadotropin treatment. At 96 h although the levels were higher but was not significantly ($p>0.05$) different from the 24 h time point. Total JNK-1 levels were not different from the 24 h time point except for a slightly higher level at 72 h. Total JNK-2 could not be detected in the granulosa cells using the conditions described in materials and methods section, while it can be detected in the monkey corpus luteum tissue (Yadav *et al.* 2002). Phospho-JNK-2 levels increased similar to p-JNK-1 levels at all time points compared to the 24 h time point (data not shown). In vitro kinase assay performed on granulosa cells retrieved at 24 and 72 h after stopping of gonadotropin treatment showed increased p-JNK activity at 72 h compared to 24 h confirming the immunoblot analysis data.

Figure 7B shows representative immunoblots and integrated arbitrary densitometric unit data of p-p38 and total p38 levels. Phsopho-p38 levels were significantly increased ($p<0.05$) in granulosa cell lysates collected at 48 and 72 h after stopping gonadotropin treatment. At 96 h, the level did not increase compared to the 24 h time point. Total p38 levels tended to be higher ($p>0.05$) at 48 and 72 h. In vitro kinase assay performed for granulosa cell lysates at 24 and 72 h revealed increased activity at 72 compared to 24 h time point.

DISCUSSION

Although rhesus monkeys undergoing controlled ovarian stimulation cycles comparable to those in clinical IVF/assisted reproduction treatment protocols for induction of multiple preovulatory follicles for studying preovulatory, periovulatory or oocyte retrieval for IVF and related research have been reported [31-33], this is the first report that describes standardization of protocol for successful induction of multiple follicular growth in the bonnet monkey. In the present study, a GnRH antagonist treatment was not included in the protocol as is reported by others (for example [31, 33]) to rule out the possibility of direct effect on the ovary. It has been shown that GnRH may have a direct effect on the ovary and may even increase the incidence of apoptosis in rat granulosa cells [34]. Interestingly, however, GnRH receptors have not been demonstrated in granulosa cells of human preovulatory follicles, but luteinized granulosa cells appear to have specific binding sites for GnRH [35].

Studies carried out in rodent, primate and a number of farm animal species have established that unwanted ovarian somatic and germ cells are eliminated by the process of apoptosis (reviewed in [1, 2, 36]). Ovarian follicular atresia in all vertebrates studied to date is mediated via apoptosis that involves well organized morphological and biochemical processes characterized by membrane blebbing, cell shrinkage, oligonucleosome formation and apoptotic bodies (reviewed in [1, 3, 37]). In the present study we investigated the feasibility of studying apoptosis in monkey granulosa cells for purposes of delineating intracellular signaling events associated with initiation of apoptosis. Prior to this study reports on granulosa cell apoptosis in human and non-human primate were scarce [25, 36]. After having established a procedure for induction

of multiple preovulatory follicles in the monkey, we then determined the time course of appearance of DNA oligonucleosomal formation in granulosa cells following withdrawal of exogenous gonadotropins, since formation of typical “DNA ladder” is considered a biochemical hallmark of apoptosis. Several studies have suggested that LMW DNA fragmentation precede or occurs coincident with morphological changes of apoptosis [38-40]. However, it has been observed that a small percentage of histologically early atretic ovarian follicles was not accompanied by DNA laddering [40]. On the other hand, it has been suggested that apoptotic process of cells characterized by chromatin condensation, reduced cell volume and formation of apoptotic cell bodies can proceed in the absence of oligonucleosomal formation, and in other situations the formation of LMW fragments occur only subsequent to the cleavage of genomic DNA into at least two different pools of high molecular weight fragments, 50 kb and 300 kb [41-43]. We assessed the time of onset of apoptosis on the basis of biochemical DNA analysis, since morphological assessment of apoptosis in a previous study correlated well with the appearance of LMW DNA fragments [23]. Moreover, the biochemical analysis appears to be a reliable index for determining the time of onset of apoptosis. In the present study as the granulosa cells did not show evidence of differentiation and since their steroid biosynthetic machinery was severely compromised, the cells began to show evidence of DNA fragmentation following clearance of exogenous gonadotropins due to metabolism. In an elegant study by Nahum et al. [39], DNA degradation in rat granulosa cells of preovulatory follicles was observed within 8 h after hypophysectomy, but in this study DNA degradation was not observed until 48 h after stopping of gonadotropin treatment. This is not surprising since exogenously administered gonadotropin preparations used in this study have

circulating biological half-life in excess of 20 h which is in contrast to perhaps a rapid clearance of endogenous gonadotropins after hypophysectomy in rats. Also, it should be pointed out that E_2 secretion continued to increase and was highest at 24 h after stopping of gonadotropin treatment, indicating that the effect of exogenously administered gonadotropins was still present after stopping treatment.

Great strides have been made in recent years towards a better understanding of events that occur in ovarian follicles following initiation of apoptosis, but the exact sequence of events responsible for triggering apoptosis in granulosa cells is still poorly understood. One key group of intracellular factors regulating apoptosis is the Bcl-2 family of proteins (reviewed in [11, 44]). Members of ever increasing mammalian Bcl-2 family currently number in excess of 20, and encode proteins that are classified as either anti-apoptotic (such as Bcl-2 and Bcl-X_L) or pro-apoptotic (such as Bax and Bad) are important in the decision step of apoptosis [2, 11]. We unsuccessfully tried to examine the expression of Bcl-X_L by RT-PCR (data not shown) with the published primers, but the reason/s for lack of expression was not clear. We next examined the expression of Bax in granulosa cells at different time intervals after stopping of gonadotropin treatment. Although in granulosa cells collected at 48 h after stopping of gonadotropin treatment a significant increase was not observed, but Bax expression increase paralleled the LMW DNA fragmentation result, a observation that corroborate the findings in the human ovary [25]. Interestingly, our attempts to determine the Bax protein expression was not successful, and Kugu et al. [25] also could not detect the protein in the atretic follicles. It could be that the Bax antibody used may not be suitable for detecting the protein in monkey tissues. Nevertheless, that Bax plays an important role in granulosa cells

apoptosis is further reinforced by the reported observation of decreased Bax expression associated with the inhibition of equine chorionic gonadotropin-mediated granulosa cell apoptosis [6]. Caspases represent a family of intracellular cysteine proteases, the actions of which are linked to the initiation and executionery phase of apoptosis (reviewed in [37]). We examined the expression pattern of two of the caspases, caspase-2 and caspase-3, both of which are involved in the penultimate stage of apoptosis. It is well established that caspase-3 is involved in virtually all types of vertebrate cell apoptosis (reviewed in [45]). Surprisingly, only marginal increase in caspase-3 mRNA levels was observed in granulosa cells undergoing apoptosis. It could be that more than the expression, it is the activity levels of caspase-3 *i.e.,* cleaved caspase–3 protein levels that is important for apoptosis. We also examined the expression of caspase-2 with a view to correlate its activity with LMW DNA fragmentation. Unlike the caspase-3 expression, a clear cut increase in the caspase-2 expression was associated with the increase in LMW DNA fragments suggesting its involvement in granulosa cell apoptosis. It has been reported that oocytes lacking caspase-2 are resistant to apoptosis in caspase-2 deficient mice [46]. Kugu et al. [25] also found increased expression of caspase-2 in apoptotic human granulosa cells. The extent of caspase-2 involvement and delineation of its intracellular apoptotic cascade need to be investigated.

The role of both FSH and LH/hCG in suppression of ovarian follicular atresia in vivo and in vitro is well established (for review see [3, 47]). Since follicles are also exposed to large number of substances such as growth factors, cytokines, hormones etc, in vivo it is possible the presence (or withdrawal) of these factors either alone or in combination may activate the apoptotic signaling cascades [3, 48]. In this regard, it has

been reported that elements of extrinsic (receptor-mediated) apoptotic signaling cascade such as Fas and Fas-L are expressed in granulosa cells following gonadotropin withdrawal (reviewed in [3]). In a recent study [49], it was conclusively demonstrated that under in vitro follicle culture conditions, FSH stimulated X-linked inhibitor of apoptosis (X-IAP) and that adenoviral X-IAP sense cDNA expression in granulosa cells reduced apoptosis suggesting that at least one of the consequences of FSH withdrawal is the reduced expression of X-IAP from thecal cells leading to apoptosis. However, it is possible that withdrawal of gonadotropin support to follicles lead to activation of multiple signaling apoptotic cascades.

Many extracellualr stimuli are converted into specific cellular responses through activation of MAP kinase signaling pathways [12]. It has been observed that serum withdrawal stress often involves activation of JNK and p38 [14]. In the present study, phosphorylated levels of JNK and p38 and ERK-2 levels were higher following withdrawal of gonadotropin treatment coinciding with the onset of LMW DNA fragments. However, in eCG-induced granulosa cell apoptosis in rats, it was reported that ERK signaling pathway was attenuated [50]. The reason for discrepancy between the monkey (although in vitro kinase assay result did not confirm the increase in the ERK activity) and rat results is not clear, but in the rat study [50] the phospho- ERK levels were lower at 48 h in the absence of LMW DNA fragments and continued to be lower at 96-120 h when LMW DNA fragments were present. We have observed increased pERK levels in rat granulosa cells 48 h after eCG treatment which decreased at 96 h, but the levels increased again at 120 h after treatment [51]. Recently, apoptosis induced by hydrogen peroxide in porcine granulosa cells in vitro showed increased phospho-ERK

levels [17]. More studies are required to further determine the exact role of ERK signaling pathway. The findings that phosphorylated JNK and p38 levels were elevated suggest that deprival of gonadotrophic support to granulosa cells resulted in stress – induced activation of MAP kinase activity indicative of their critical role during apoptosis.

In summary, the studies reported here demonstrate that monkey granulosa cells of preovulatory follicles undergo apoptosis following withdrawal of gonadotropin support. Moreover, MAP kinases appear to be activated during granulosa cell apoptosis. Future studies will be aimed at delineation of MAP kinase activated pathways associated with initiation of apoptosis.

ACKNOWLEDGMENTS

We are grateful to Dr. S. G. Ramachandra of Primate Research Laboratory for help with surgeries and Mr. Vijay Kumar Yadav for help with in vitro MAP kinase assays. Dr. A. F. Parlow kindly supplied the monkey LH RIA kit.

REFERENCES

1. Kaipia A, Hsueh AJ. Regulation of ovarian follicle atresia. Annu Rev Physiol 1997; 59:349-363.
2. Martimbeau S, Tilly JL. Physiological cell death in endocrine-dependent tissues: an ovarian perspective. Clin Endocrinol (Oxf) 1997; 46:241-254.
3. Jiang JY, Cheung CK, Wang Y, Tsang BK. Regulation of cell death and cell survival gene expression during ovarian follicular development and atresia. Front Biosci 2003; 8:222-237.
4. Hughes FM Jr, Gorospe WC. Biochemical identification of apoptosis (programmed cell death) in granulosa cells: evidence for a potential mechanism underlying follicular atresia. Endocrinology 1991; 129:2415-2422.
5. Hakuno N, Koji T, Yano T, Kobayashi N, Tsutsumi O, Taketani Y, Nakane PK. Fas/APO-1/CD95 system as a mediator of granulosa cell apoptosis in ovarian follicle atresia. Endocrinology 1996; 137:1938-1948.
6. Tilly JL, Tilly KI, Kenton ML, Johnson AL. Expression of members of the bcl-2 gene family in the immature rat ovary: equine chorionic gonadotropin-mediated inhibition of granulosa cell apoptosis is associated with decreased bax and constitutive bcl-2 and bcl-xlong messenger ribonucleic acid levels. Endocrinology 1995; 136:232-241.
7. Tajima K, Orisaka M, Hosokawa K, Amsterdam A, Kotsuji F. Effects of ovarian theca cells on apoptosis and proliferation of granulosa cells: changes during bovine follicular maturation. Biol Reprod 2002; 66:1635-1639.

8. Hsueh AJ, McGee EA, Hayashi M, Hsu SY. Hormonal regulation of early follicle development in the rat ovary. Mol Cell Endocrinol 2000; 163:95-100.
9. McGee EA, Hsueh AJ. Initial and cyclic recruitment of ovarian follicles. Endocr Rev 2000; 21:200-214.
10. Findlay JK, Drummond AE, Dyson ML, Baillie AJ, Robertson DM, Ethier JF. Recruitment and development of the follicle; the roles of the transforming growth factor-beta superfamily. Mol Cell Endocrinol 2002; 191:35-43.
11. Hsu SY, Hsueh AJ. Tissue-specific Bcl-2 protein partners in apoptosis: An ovarian paradigm. Physiol Rev 2000; 80:593-614.
12. Pearson G, Robinson F, Beers Gibson T, Xu BE, Karandikar M, Berman K, Cobb MH. Mitogen-activated protein (MAP) kinase pathways: regulation and physiological functions. Endocr Rev 2001; 22:153-183.
13. Xia Z, Dickens M, Raingeaud J, Davis RJ, Greenberg ME. Opposing effects of ERK and JNK-p38 MAP kinases on apoptosis. Science 1995; 270:1326-1331.
14. Kummer JL, Rao PK, Heidenreich KA. Apoptosis induced by withdrawal of trophic factors is mediated by p38 mitogen-activated protein kinase. J Biol Chem 1997; 272:20490-20494.
15. Maizels ET, Cottom J, Jones JC, Hunzicker-Dunn M. Follicle stimulating hormone (FSH) activates the p38 mitogen-activated protein kinase pathway, inducing small heat shock protein phosphorylation and cell rounding in immature rat ovarian granulosa cells. Endocrinology 1998; 139:3353-3356.
16. Babu PS, Krishnamurthy H, Chedrese PJ, Sairam MR. Activation of extracellular-regulated kinase pathways in ovarian granulosa cells by the novel growth factor type 1

follicle-stimulating hormone receptor. Role in hormone signaling and cell proliferation. J Biol Chem 2000; 275:27615-27626.

17. Shiota M, Sugai N, Tamura M, Yamaguchi R, Fukushima N, Miyano T, Miyazaki H. Correlation of mitogen-activated protein kinase activities with cell survival and apoptosis in porcine granulosa cells. Zoolog Sci 2003; 20:193-201.
18. Srinath, BR. Husbandry and breeding of bonnet monkeys (*Macaca radiata*). In: Anand Kumar TC (ed.), Non-human Primate Models for the Study of Human Reproduction. Basel: S.Karger; 1979: 17-22.
19. Zelinski-Wooten MB, Alexander M, Christensen CL, Wolf DP, Hess DL, Stouffer RL. Individualized gonadotropin regimens for follicular stimulation in macaques during in vitro fertilization (IVF) cycles. J Med Primatol 1994; 23:367-374.
20. Wolf DP, Thomson JA, Zelinski-Wooten MB, Stouffer RL. IVF-ET in old world monkeys. In: Brenner RL, Stouffer RL, Wolf DP (eds.), In-Vitro Fertilization and Embryo Transfer in Primates. New York: Springer-Verlag; 1993: 85-99.
21. Yadav VK, Medhamurthy R. Developmental regulation of Mitogen-activated protein (MAP) kinases in corpus luteum: changes during luteolysis and simulated early pregnancy in the bonnet monkey. In: Program of 84th Annual Meeting of the Endocrine society; 2002; San Francisco, CA. Abstract 415.
22. Tilly JL, Hsueh AJ. Microscale autoradiographic method for the qualitative and quantitative analysis of apoptotic DNA fragmentation. J Cell Physiol 1993; 154:519-526.
23. Yadav VK, Sudhagar RR, Medhamurthy R. Apoptosis during spontaneous and prostaglandin $F_{2\alpha}$–induced luteal regression in the buffalo cow (*Bubalus bubalis*): involvement of mitogen-activate protein kinases. Biol Reprod 2002; 67:752-759.

24. Wong H, Anderson WD, Cheng T, Riabowol KT. Monitoring mRNA expression by polymerase chain reaction: the "primer-dropping" method. Anal Biochem 1994; 223:251-258.

25. Kugu K, Ratts VS, Piquette GN, Tilly KI, Tao XJ, Martimbeau S, Aberdeen GW, Krajewski S, Reed JC, Pepe GJ, Albrecht ED, Tilly JL. Analysis of apoptosis and expression of bcl-2 gene family members in the human and baboon ovary. Cell Death Differ 1998; 5:67-76.

26. Mazerbourg S, Overgaard MT, Oxvig C, Christiansen M, Conover CA, Laurendeau I, Vidaud M, Tosser-Klopp G, Zapf J, Monget P. Pregnancy-associated plasma protein-A (PAPP-A) in ovine, bovine, porcine, and equine ovarian follicles: involvement in IGF binding protein-4 proteolytic degradation and mRNA expression during follicular development.

Endocrinology 2001; 142:5243-5253.

27. Bradford MM. A rapid and sensitive method for the quantitation of microgram quantities of protein utilizing the principle of protein-dye binding. Anal Biochem 1976; 72:248-254.

28. Yamauchi J, Kaziro Y, Itoh H. Differential regulation of mitogen-activated protein kinase kinase 4 (MKK4) and 7 (MKK7) by signaling from G protein beta gamma subunit in human embryonal kidney 293 cells. J Biol Chem 1999; 274:1957-1965.

29. Kuroki DW, Minden A, Sanchez I, Wattenberg EV. Regulation of a c-Jun amino-terminal kinase/stress-activated protein kinase cascade by a sodium-dependent signal transduction pathway. J Biol Chem 1997; 272:23905-23911.

30. Selvaraj N, Medhamurthy R, Ramachandra SG, Sairam MR and Moudgal NR. Assessment of Luteal Rescue and Desensitization of Macaque corpus luteum brought about by human chorionic gonadotrophin and deglycosylated human chorionic gonadotrophin treatment. J Biosci 1996; 21:497-510.
31. Chandrasekher YA, Hutchison JS, Zelinski-Wooten MB, Hess DL, Wolf DP, Stouffer RL. Initiation of periovulatory events in primate follicles using recombinant and native human luteinizing hormone to mimic the midcycle gonadotropin surge. J Clin Endocrinol Metab 1994; 79:298-306.
32. Stouffer RL. Pre-ovulatory events in the rhesus monkey follicle during ovulation induction. Reprod Biomed Online 2002; 4 (Suppl 3):1-4.
33. Martinez-Chequer JC, Stouffer RL, Hazzard TM, Patton PE, Molskness TA. Insulin-like growth factors-1 and -2, but not hypoxia, synergize with gonadotropin hormone to promote vascular endothelial growth factor-a secretion by monkey granulosa cells from preovulatory follicles. Biol Reprod 2003; 68:1112-1118.
34. Parborell F, Pecci A, Gonzalez O, Vitale A, Tesone M. Effects of a gonadotropin-releasing hormone agonist on rat ovarian follicle apoptosis: regulation by epidermal growth factor and the expression of Bcl-2-related genes. Biol Reprod 2002; 67:481-486.
35. Brus L, Lambalk CB, de Koning J, Helder MN, Janssens RM, Schoemaker J. Specific gonadotrophin-releasing hormone analogue binding predominantly in human luteinized follicular aspirates and not in human pre-ovulatory follicles. Hum Reprod 1997; 12:769-73.
36. Vaskivuo TE, Tapanainen JS. Apoptosis in the human ovary. Reprod Biomed Online 2003; 6:24-35.

37. Johnson AL, Bridgham JT. Caspase-mediated apoptosis in the vertebrate ovary. Reproduction 2002; 124:19-27.

38. Guthrie HD, Grimes RW, Cooper BS, Hammond JM. Follicular atresia in pigs: measurement and physiology. J Anim Sci 1995; 73:2834-2844.

39. Nahum R, Beyth Y, Chun SY, Hsueh AJ, Tsafriri A. Early onset of deoxyribonucleic acid fragmentation during atresia of preovulatory ovarian follicles in rats. Biol Reprod 1996; 55:1075-1080.

40. Pedersen HG, Watson ED, Telfer EE. Analysis of atresia in equine follicles using histology, fresh granulosa cell morphology and detection of DNA fragmentation. Reproduction 2003; 125:417-423.

41. Barbieri D, Troiano L, Grassilli E, Agnesini C, Cristofalo EA, Monti D, Capri M, Cossarizza A, Franceschi C. Inhibition of apoptosis by zinc: a reappraisal. Biochem Biophys Res Commun 1992; 187:1256-1261.

42. Oberhammer F, Wilson JW, Dive C, Morris ID, Hickman JA, Wakeling AE, Walker FR, Sikorsk M. Apoptotic death in epithelial cells: cleavage of DNA to 300 and/ or 50 kb fragments prior to or in the absence of internucleosomal fragmentation. EMBO J 1993; 12:3679-3684.

43. Flaws JA, Kugu K, Trbovich AM, DeSanti A, Tilly KI, Hirshfield AN, Tilly JL. Interleukin-1 beta-converting enzyme-related proteases (IRPs) and mammalian cell death: dissociation of IRP-induced oligonucleosomal endonuclease activity from morphological apoptosis in granulosa cells of the ovarian follicle. Endocrinology 1995; 136:5042-5053.

44. Marti A, Jaggi R, Vallan C, Ritter PM, Baltzer A, Srinivasan A, Dharmarajan AM, Friis RR. Physiological apoptosis in hormone-dependent tissues: involvement of caspases. Cell Death Differ 1999; 6:1190-2000.
45. Colussi PA, Kumar S. Targeted disruption of caspase genes in mice: what they tell us about the functions of individual caspases in apoptosis. Immunol Cell Biol 1999; 77:58-63.
46. Bergeron L, Perez GI, Macdonald G, Shi L, Sun Y, Jurisicova A, Varmuza S, Latham KE, Flaws JA, Salter JC, Hara H, Moskowitz MA, Li E, Greenberg A, Tilly JL, Yuan J. Defects in regulation of apoptosis in caspase-2-deficient mice. Genes Dev 1998; 12:1304-1314.
47. Hsueh AJ, Billig H, Tsafriri A. Ovarian follicle atresia: a hormonally controlled apoptotic process. Endocr Rev 1994; 15:707-724.
48. Tilly JL, Billig H, Kowalski KI, Hsueh AJ. Epidermal growth factor and basic fibroblast growth factor suppress the spontaneous onset of apoptosis in cultured rat ovarian granulosa cells and follicles by a tyrosine kinase-dependent mechanism. Mol Endocrinol 1992; 6:1942-1950.
49. Wang Y, Rippstein PU, Tsang BK. Role and gonadotrophic regulation of X-linked inhibitor of apoptosis protein expression during rat ovarian follicular development in vitro. Biol Reprod 2003; 68:610-619.
50. Gebauer G, Peter AT, Onesime D, Dhanasekaran N. Apoptosis of ovarian granulosa cells: correlation with the reduced activity of ERK-signaling module. J Cell Biochem 1999; 75:547-554.

51. Medhamurthy R, Muraly P, Uma J. Role of mitogen activated protein kinases during ovarian follicular growth and apoptosis. In: National Conference on Recent Advances in Reproductive Health; 2003; Jaipur, India. pp 170.

Figure Legends

Figure 1. Serum estradiol levels before, during exogenous gonadotropin treatment (6 days of hFSH preparation (25 IU twice daily) followed by 2.5 days of a combination of hFSH and hLH preparation (25 IU twice daily), and after stopping of gonadotropin treatment in bonnet monkeys. The open and solid bars represent duration of hFSH and hFSH plus hLH treatments, respectively. The data is represented as mean ± SEM, n=15 monkeys on days 1-9 of gonadotropin treatment, n=15 (24 h), n=9 (48 h), n=6 (72 h) and n=3 (96 h) monkeys at different time intervals after stopping of treatment. For analysis details see Fig.3.

Figure 2. Follicular fluid estradiol (▭) and progesterone (▬) concentrations at different time intervals after stopping of gonadotropin treatment. Bars with different letters are different ($p<0.05$) from each other.

Figure 3. Serum estradiol (●—●)and progesterone (▲—▲) concentrations after stopping of gonadotropin treatment. Based on pattern of follicular fluid and serum levels of estradiol and progesterone, the follicular growth period is divided into two phases viz: proliferative (left panel) and non- proliferative phase (right panel). Please note that serum progesterone levels remained low during the non-proliferative phase that indicated of absence of differentiation of granulosa cells. The time points with different letters are different ($p<0.05$) from each other.

Figure 4. Analysis of apoptotic DNA fragmentation in granulosa cells. Genomic DNA isolated from monkey granulosa cells retrieved from preovulatory follicles at different time intervals after stopping exogenous gonadotropin treatment was subjected to either qualitative (A) or quantitative (B) analysis. M indicates a 100 base pair ladder. Bar graph (C) represents the quantitative measurement of low molecular weight DNA labeling as a percentage of change from 24 h time point. Bars with different letters above them are significantly different ($p < 0.05$).

Figure 5. Bax (A), caspase-2 (▬) and caspase-3 (▭) (B) mRNA expression in the monkey granulosa cells retrieved from follicles at different time intervals after stopping of gonadotropin treatment. mRNA of Bax and caspase-2 and caspase-3 were co-amplified with the internal standard ribosomal acidic phosphoprotein (RPLO), an constitutive house keeping gene and intensities of the amplified Bax, caspase-2 and caspase-3 products were normalized against the internal standard. M indicates a 100 base pair ladder. A representative gel is shown for Bax (A), caspase-2 and caspase-3 (B) mRNAs. Due to lack of availability of sufficient RNA in few of the monkeys, the densitometric data represented for caspase-2 and -3 is an average of two monkeys/time point with no statistical analysis performed on the data (Fig. 5B). Bars with different letters are significantly different ($p<0.05$).

Figure 6. Autoradiographic analysis of phospho GST-Elk-1 and immunoblot analyses of phospho ERK-1 and -2 (▭) and total ERK-1 and -2 (▬) in protein lysates of granulosa cells retrieved from follicles at different intervals after stopping of gonadotropin treatment. The blots shown are from one of the three independent experiments (granulosa cells from one monkey from each time point was used per experiment). The arbitrary

densitometric units from 24 h time point were set as 100%, and results at other time points were expressed in relation to the 24 h value. In vitro ERK kinase (phospho-Elk-1) was performed on only two time points.

Figure 7. Autoradiographic analysis of phospho GST-c-jun and immunoblot analyses of pJNK-1 (▭) and 2 and total JNK1 (■) (panel A); phospho-ATF2, phospho-p38MAPK (pp38) (▭)and total p38 (▭) (panel B) in protein lysates of granulosa cells retrieved from follicles at different intervals after stopping of gonadotropin treatment. The blots shown are from one of three independent experiments (granulosa cells from a single monkey from each time point was used per experiment).

Table 1. Primer sequences used for RT-PCR analysis

Gene	Sequence	Size (bp)	Ref.
Caspase 3/CPP32	F: 5' ACATGGAAGCGAATCAATGGACTC 3'	686	[25]
	R: R: 5' AAGGACTCAAATTCTGTTGCCACC 3'		
Caspase 2/ICH1	F: 5' TGGCATATAGGTTGCAGTCTCGG 3'	362	[25]
	R: 5' TGTTCTGTAGGCTTGGGCAGTTG 3'		
Bax	F: 5' TCATCCAGGATCGAGCAGGG 3'	238	
	R: 5' ACAAAGATGGTCACGGTCTGCC 3'		
36B4, acidic ribosomal phosphoprotein (RPLO)	F: 5' GGCGACCTGGAAGTCCAACT 3'	129	[26]
	R: 5' CCATCAGCACCACAGCCTTC 3'		

Sequences were either taken from published references or designed for the current study using the program at http://www.genome.wi.mit.edu/cgi-bin/primer/primer3_www.cgi.

Fig. 1

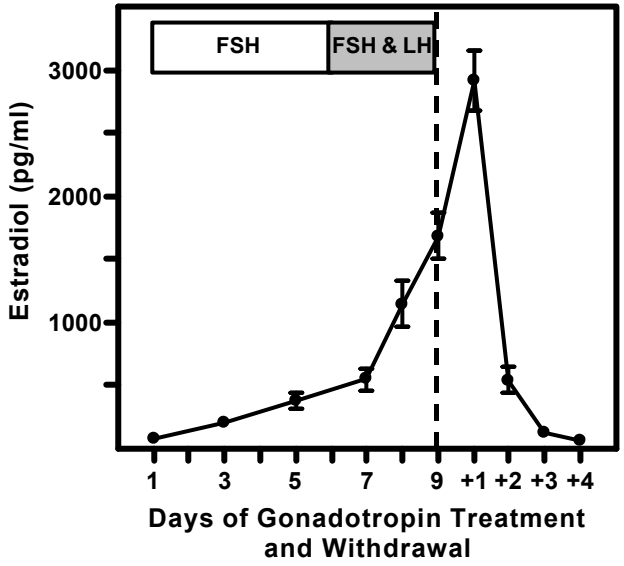
FSH
FSH & LH
3000
2000
1000
Estradiol (pg/ml)
1
3
5
7
9
+1
+2
+3
+4
Days of Gonadotropin Treatment
and Withdrawal

Fig. 2

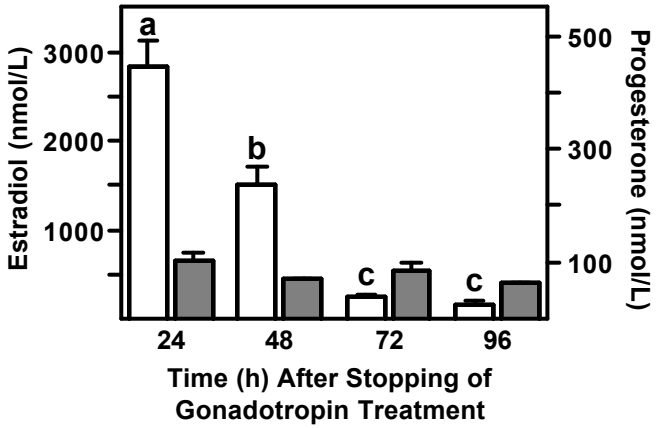
a
b
c
c
3000
2000
1000
500
300
100
Estradiol (nmol/L)
Progesterone (nmol/L)
24
48
72
96
Time (h) After Stopping of
Gonadotropin Treatment

Fig. 3

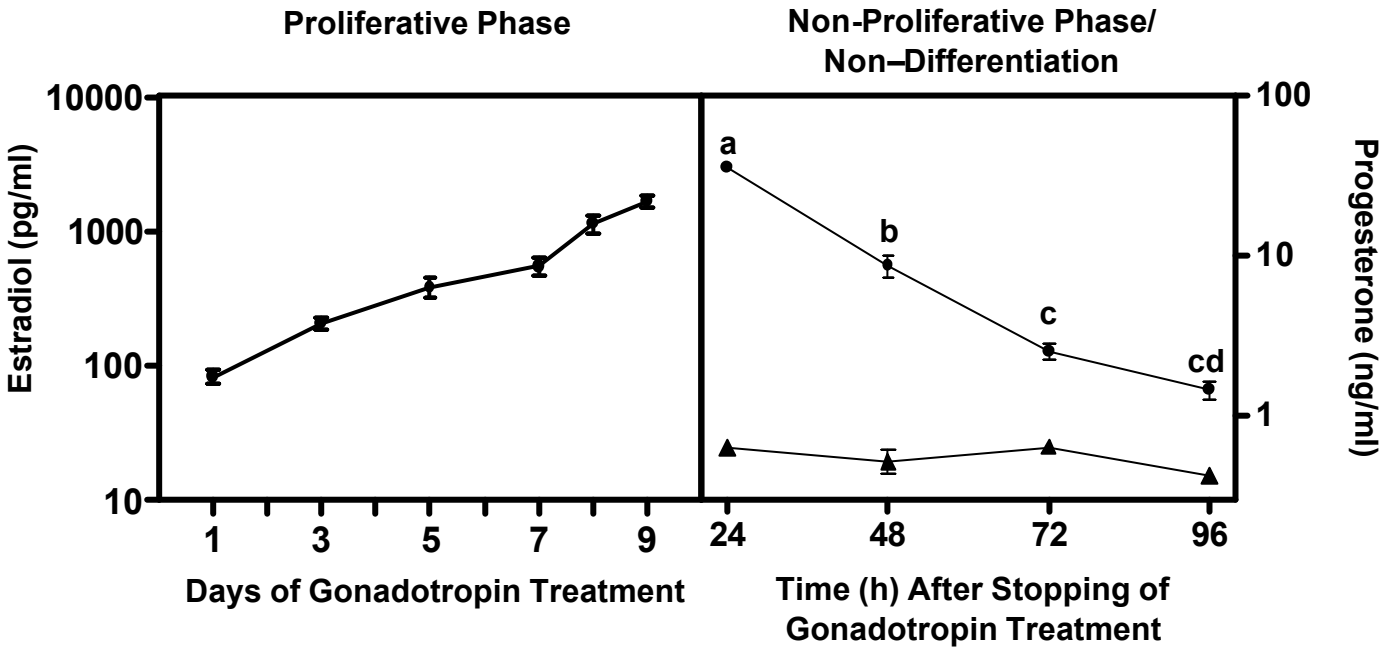
Proliferative Phase
Non-Proliferative Phase/
Non–Differentiation
10000
1000
100
10
Estradiol (pg/ml)
100
10
1
Progesterone (ng/ml)
a
b
c
cd
1
3
5
7
9
24
48
72
96
Days of Gonadotropin Treatment
Time (h) After Stopping of
Gonadotropin Treatment

Fig. 4

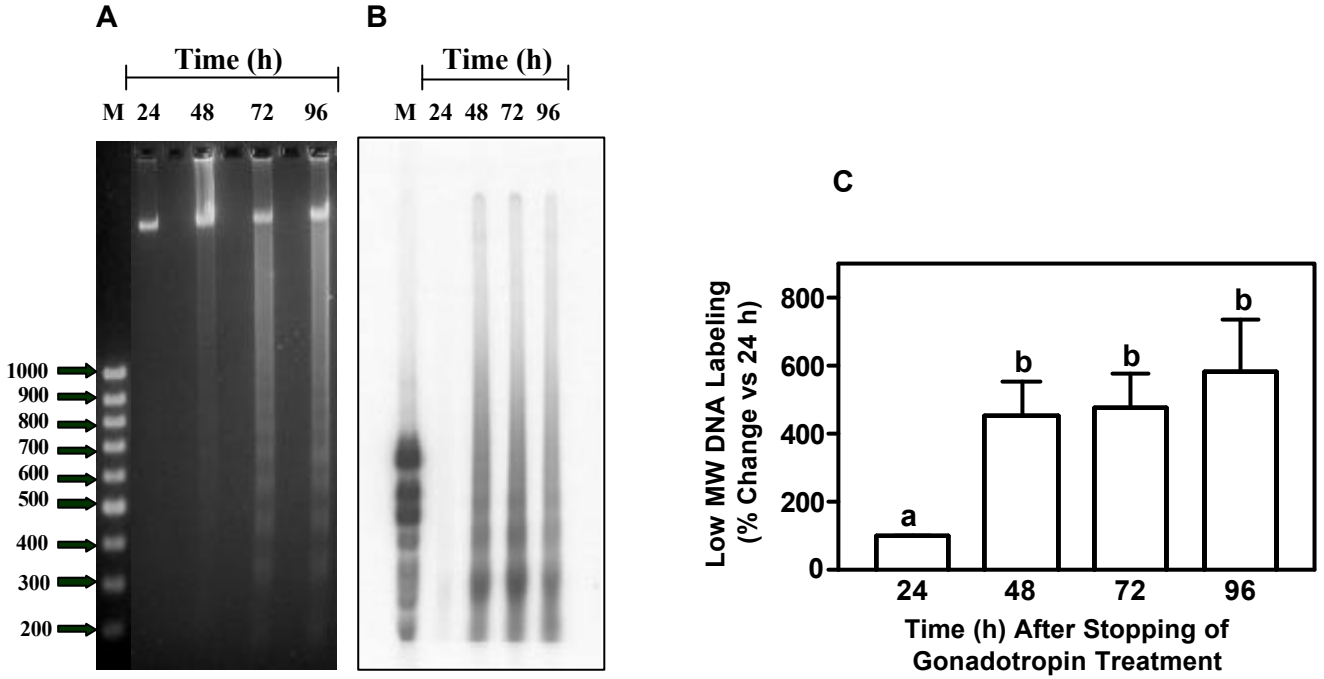
A
Time (h)
M 24 48 72 96
1000
900
800
700
600
500
400
300
200
B
Time (h)
M 24 48 72 96
C
Low MW DNA Labeling
(% Change vs 24 h)
800
600
400
200
0
a
b
b
b
24
48
72
96
Time (h) After Stopping of
Gonadotropin Treatment

Fig. 5

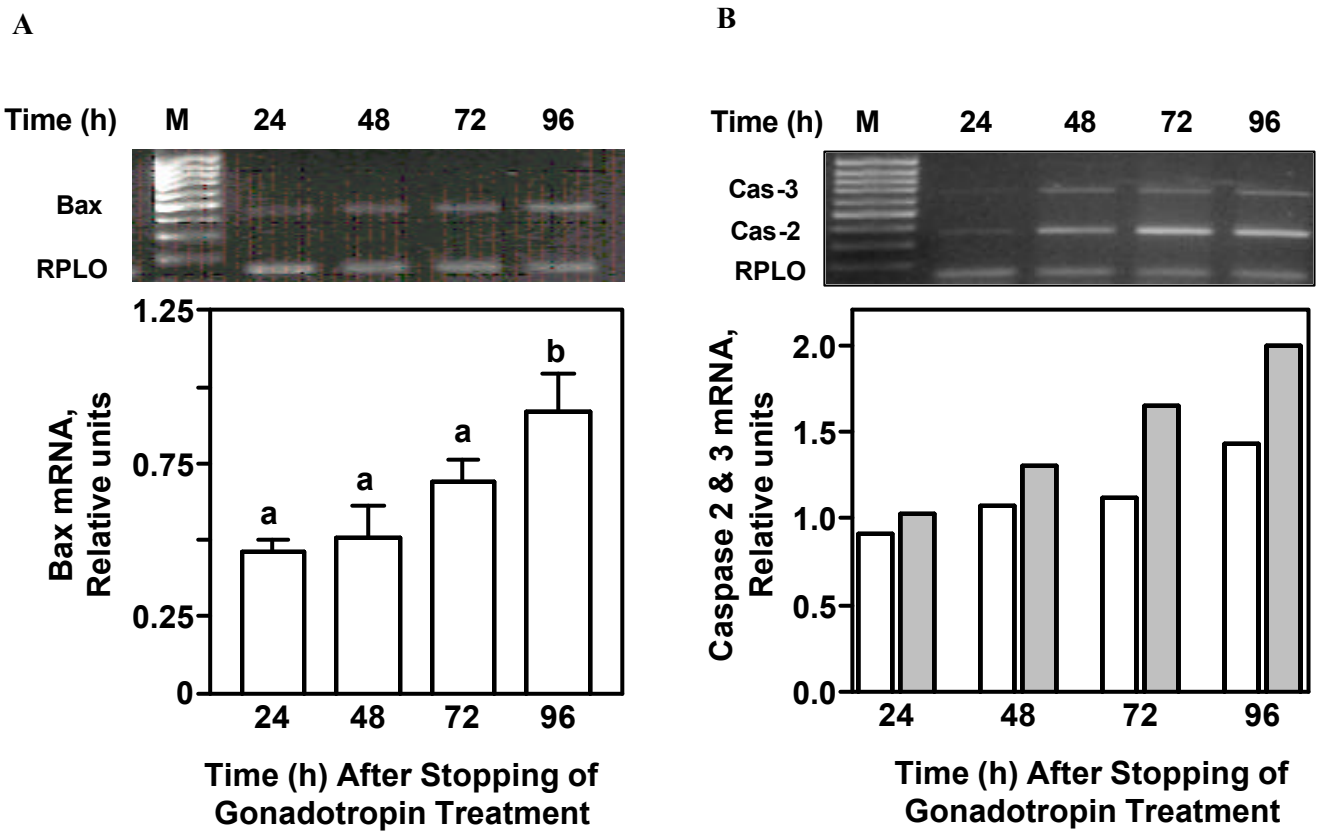
A
Time (h)
M
24
48
72
96
Bax
RPLO
Bax mRNA, Relative units
1.25
0.75
0.25
0
a
a
a
b
24
48
72
96
Time (h) After Stopping of Gonadotropin Treatment
B
Time (h)
M
24
48
72
96
Cas-3
Cas-2
RPLO
Caspase 2 & 3 mRNA, Relative units
2.0
1.5
1.0
0.5
0.0
24
48
72
96
Time (h) After Stopping of Gonadotropin Treatment

Fig. 6

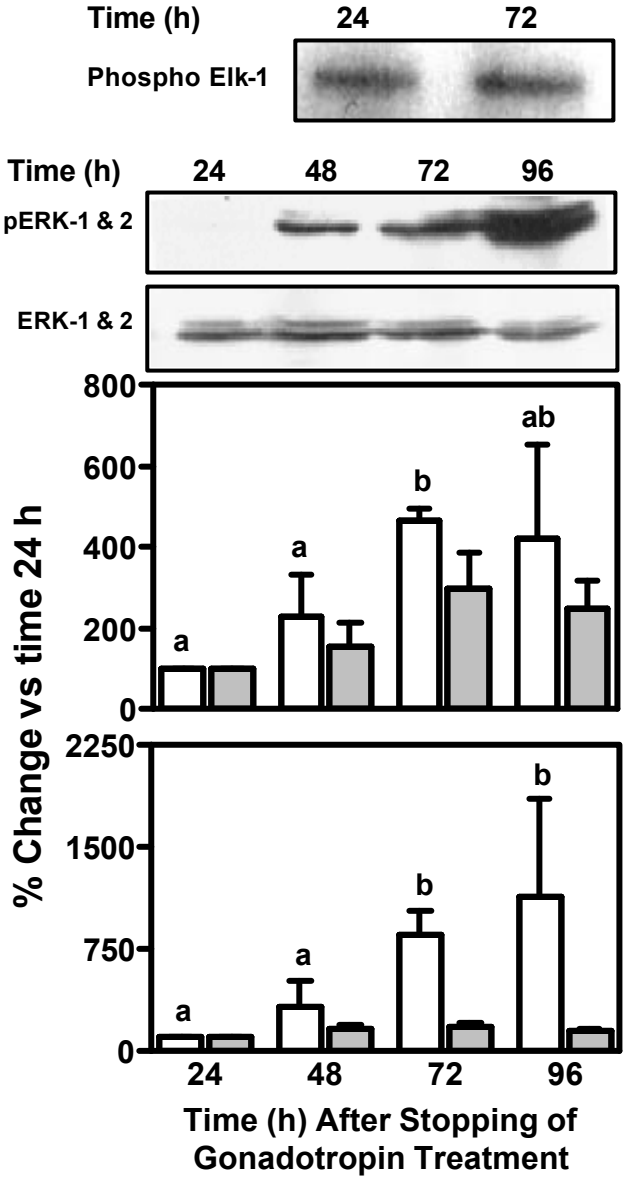
Time (h)
24
72
Phospho Elk-1
Time (h)
24
48
72
96
pERK-1 & 2
ERK-1 & 2
800
600
400
200
0
a
a
b
ab
2250
1500
750
0
a
a
b
b
% Change vs time 24 h
24
48
72
96
Time (h) After Stopping of Gonadotropin Treatment

Fig. 7

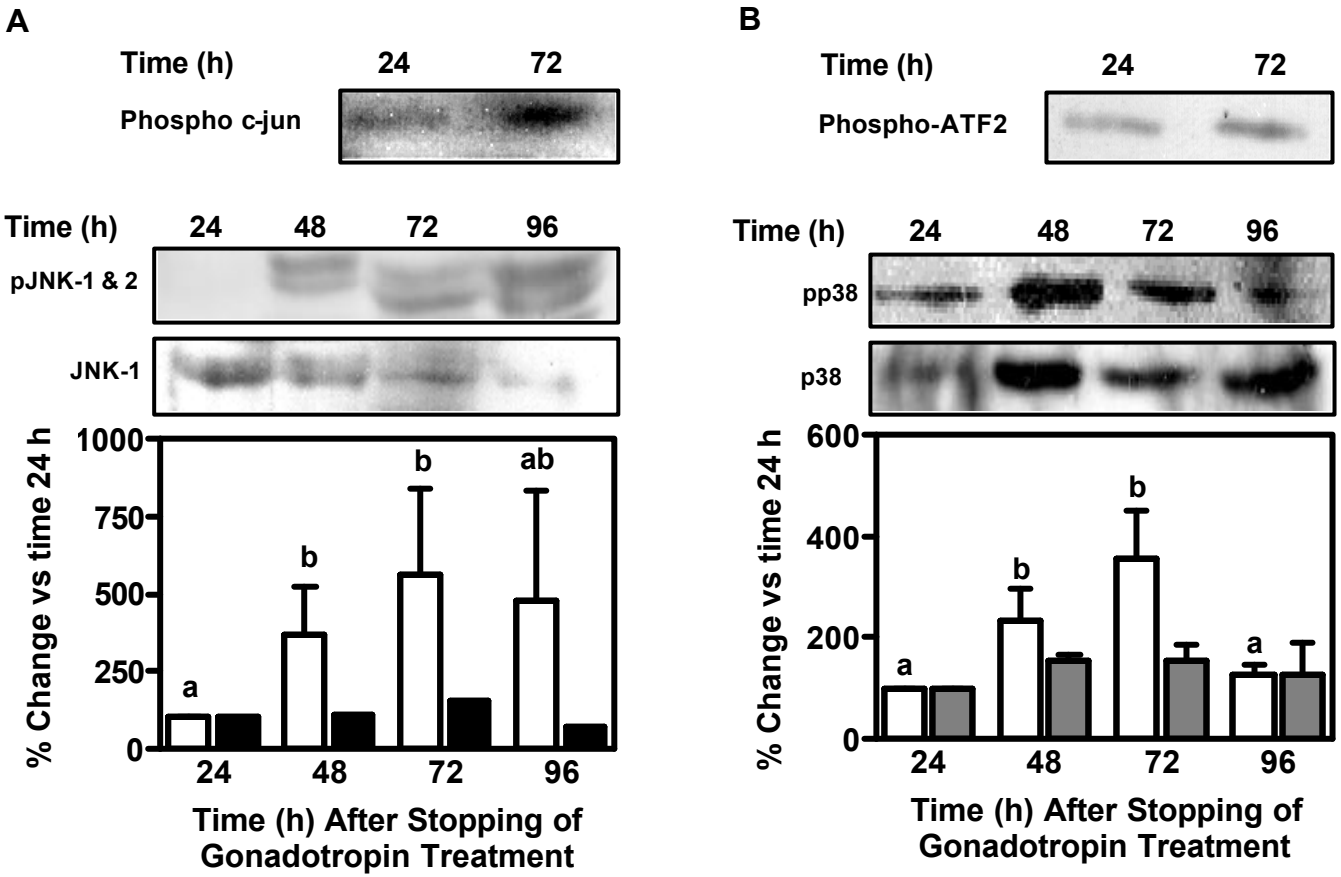
A
Time (h)
24
72
Phospho c-jun
Time (h)
24
48
72
96
pJNK-1 & 2
JNK-1
% Change vs time 24 h
1000
750
500
250
0
a
b
b
ab
24
48
72
96
Time (h) After Stopping of Gonadotropin Treatment
B
Time (h)
24
72
Phospho-ATF2
Time (h)
24
48
72
96
pp38
p38
% Change vs time 24 h
600
400
200
0
a
b
b
a
24
48
72
96
Time (h) After Stopping of Gonadotropin Treatment